Master of Science

HEAT TREATMENT AND MECHANICAL PROPERTIES OF 316L STAINLESS STEEL PRODUCED BY ADDITIVE MANUFACTURING PROCESS

The Graduate School of the University of Ulsan

School of Materials Science and Engineering

Dinh Van Cong

HEAT TREATMENT AND MECHANICAL PROPERTIES OF 316L STAINLESS STEEL PRODUCED BY ADDITIVE MANUFACTURING PROCESS

Advisor: Jin-Chun Kim

A Dissertation

Submitted to the Graduate School of the University of Ulsan

In partial Fulfillment of the Requirements

for the Degree of

Master of Science

By

Dinh Van Cong

School of Materials Science and Engineering

Ulsan, Korea

December 2020

적층공정으로 제조된 316L 스테인리스강의 열처리 및 기계적 특성분석

Heat Treatment and Mechanical Properties of 316L Stainless Steel Produced by Additive Manufacturing

This certifies that the dissertation of

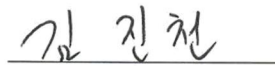Dinh Van Cong is approved

Committee Chair   Professor Sang-Yong Shin

Committee Member   Professor Jung-Gu Lee

Committee Member   Professor Jin-Chun Kim

School of Materials Science and Engineering

Ulsan, Korea

December 2020

Dinh Van Cong의 공학 석사학위 논문을 인준함

심사위원 신상용 (인)

심사위원 이정구 (인)

심사위원 김진천 (인)

울산대학교 대학원

2020 년 12 월

ACKNOWLEDGEMENT

I would like to express sincerely my thanks to my research advisor, family, friends and many others for their guidance, support and help. My research work would not have been complete without their help.

I would like to express the deepest appreciation to my research advisor Prof. Jin-Chun Kim. He continually and convincingly conveyed a spirit of adventure in regard to research, scholarship, and an excitement in regard to teaching. Without his guidance and persistent help this dissertation would not have been possible.

I also thank all member of Future Powder Materials and Processing Lab and all staffs at School of Materials Science ang Engineering for their help for the past two years.

I would never forget all the charts and wonderful moments I share with my all friends in University of Ulsan. They have encouraged and helped me in study as well as in life for two years studying in Korea. My special thanks to Mr. Do Thanh Thuong, Ms. Nguyen Thi Anh Nguyet, Mr. Tran Minh Tien, Mr. Tran Van Loi, who helped me throughout the process of the experimenting and implementing this thesis.

Last but not the least my greatest thank goes to my family for their unflagging love and conditional support throughout my studies and my life in general.

Thanks all, sincerely.

Dinh Van Cong

TABLE OF CONTENTS

LIST OF FIGURES

LIST OF TABLES

PREFACE

316L stainless steel is a type of molybdenum bearing austenitic stainless steel. This steel has a lower carbon and higher molybdenum of percentage than 316 stainless steel. The maximum carbon content in this steel composition is 0.03%, which minimizes the precipitation of carbide during welding. This steel is characterized by high creep resistance, excellent corrosion and pitting resistance, and excellent formability, etc. As a result, this steel is widely used in many industries and commerce, especially in shipbuilding industry and marine.316L stainless steel parts are produced by traditional methods like forging, casting or extrusion, etc. However, these methods do not allow manufacture parts with complex shapes, and the product has to be weld or machined into final form. Therefore, the production processes are time consuming and costly. In the present, a new technology has solved the issue to an extent in certain application regarding to complex shapes and monolithic structure. This is additive manufacturing (AM) technique. However, there are many limitations in the understanding structure and mechanical properties of additive manufactured components.

AM is a new technology that fabricates three-dimensional objects through using a computer-aided design (CAD) model or a digital 3D mode [3]. Powder bed fusion (PBF) process is one of the main metallic AM technologies, during which one or multiple laser manner [4]. PBF process spread powdered material over the previously joined layer, ready for processing of the next layer hence the manufacturing is discrete rather than continuous [5]. Each layer is then sequentially bonded on top of each other. The quality of product fabricated by PBF method will depend on the parameters such as laser scanning speed, laser power, layer thickness, hatch distance, laser orientation and build-direction. Therefore, PBF process is a parameter sensitive process.

This study aims to better understanding the effect of process parameters and the heat treatment on microstructure and mechanical properties of 316L stainless steel specimens produced by PBF process. Tensile and Vickers hardness test were conducted to study the evolution in mechanical properties after applying different experimental conditions.

<div align="center">**CHAPTER 1 – LITERATURE REVIEW**</div>

1.1. Additive manufacturing

1.1.1. Introduction

Additive manufacturing (AM) or 3D printing is new technology, which builds the objects have three-dimension from a digital 3D model or a computer- aided design (CAD) model [1]. The term "AM" or "3D" regard to many processes in which a three-dimension object is created by depositing, joining, solidifying original material under computer control [2]. In these processes, materials will be added together such as powder grains or liquid molecules being fused, and typically follow principle layer by layer.

 AM techniques began to appear with the name "rapid prototyping" in the 1980s [3]. During that time, these techniques were considered only suitable for manufacture of aesthetic or functional prototypes. As of 2019, some AM processes were considered as an industrial production technology because of an increasing at high level of material range, the repeatability and precision. Accordingly, the term additive manufacturing could be used as equivalent to 3D printing. One of the greatest features AM is its ability to make very complex geometries or shapes that cannot created by hand, consisting of hollow parts or objects have internal structures for the purpose of reducing mass. The most commonly used AM process in 2020 is fused deposition modeling (FDM) [4].

1.1.2. General principles

In the first stage of AM processes, objects need to be simulated into 3D models using a CAD package via a 3D scanner or by photogrammetry software and a plain digital camera. 3D printed parts created using 3D models with CAD package give better results than other methods. Before printing, the 3D printable models can be identified errors and corrected them [5]. The preparation of geometric data for 3D computer graphic via a manual modeling process is similar shaping arts as sculpting. 3D scanning process is a collecting digital data process about the appearance and shape of a real object to create a digital model base on it.

3D digital models with CAD can be save in the additive manufacturing file format (AMF) or stereolithography file format (STL). STL is a de facto file format for additive manufacturing. It stores digital data. However, STL is not designed exclusively for additive manufacturing because it produces large file sizes of parts and optimized topology due to the large number of related surfaces. To solve that problem, a new CAD file format was introduced in 2011, that is additive manufacturing file format (AMF). AMF stores data by using curve triangulations [6].
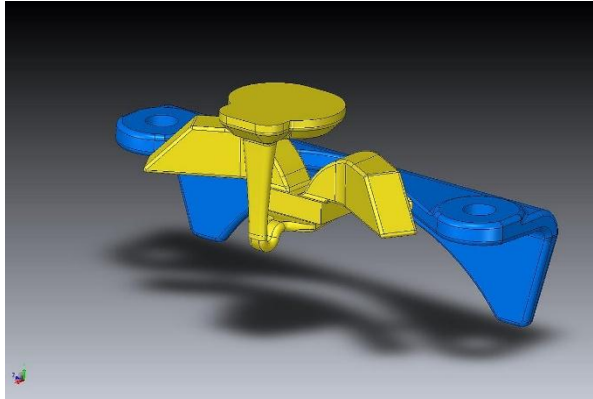
Figure 1. CAD model used for 3D printing [41]

The STL must be checked for errors before printing 3D models. All of most CAD applications generate errors in the output STL file [7]. These errors are usually of the following types:

- holes
- faces normal
- self-intersections
- noise shells
- manifold errors [8].

One step in the STL generation called "repair" fixes such errors in the original model [9]. In general, STLs are generated from a model obtained by 3D scanning generally have more these errors [10] because 3D scanning is usually achieved by point-to-point mapping/acquisition. The reconstruction of 3D models is often at fault.

After completing, a piece of software called a "slicer" process the STL files. This software converts the 3D model into a set of thin layers and generates a G code file including suitable instruction for a specific kind of 3D printer [11].

Printer resolution describes layer thickness and X–Y resolution in dots per inch (dpi) or micrometers (μm). Typical layer thickness is around 100 μm (250 DPI), although some machines can print layers as thin as 16 μm (1,600 DPI) [12]. X–Y resolution is comparable to that of laser printers. The particles (3D dots) are around 50 to 100 μm (510 to 250 DPI) in diameter. For that

printer resolution, specifying a mesh resolution of 0.01–0.03 mm and a chord length $\leq$ 0.016 mm generate an optimal STL output file for a given model input file [13]. Specifying higher resolution results in larger files without increase in print quality.

Depending upon the method used and the dimension and complexity of the model, the design of a model using contemporary methods will last from several hours to several days. Additional devices will usually reduce this time to several hours, but the equipment used, and the size and number of models being manufactured at the same time vary greatly.

Although the resolution provided by the printer can be enough for many applications, a slightly overflowing version of the required object can be printed in standard resolution, which then eliminates the material using the subtractive method of higher resolution[14].

The layered structure of each method of additive production would eventually result in an escalating effect on the piece surfaces which in relation to the building platform are curved or inclined. The effects depend heavily on a partial surface 's orientation inside the building phase [15].

Some printable polymers, such as ABS, make the surfacing smooth and enhance using acetone and other related solvent chemical vapor processes.

Some AM techniques can be used in the construction of several materials. These methods can be printed simultaneously in several colors and color variations and do not need to be painted necessarily.

Some printing techniques include the installation of internal supports for overhanging features. The media must be removed or dissolved mechanically after printing is finished.

All commercialized 3D metal printers enable the metal portion to be cut off after deposition from the metal substratum. A new GMAW 3D printing method allows the aluminum [16] or steel surface changes to the substrates [17] to be eliminated.

1.1.3. Classification of AM processes

The branded AM processes are various and can be divided into 7 categories:

- Vat photopolymerization
- Material jetting
- Binder jetting
- Powder bed fusion
- Material extrusion

- Directed energy deposition

- Sheet lamination

The main differences between processes are in the way layers are stored to produce components and the materials used. Each process has its own benefit and disadvantages, such that some companies give the material used in the construction of the object an option of powder and polymer [18]. Often some people use regular off-shelf papers to create a robust prototype as building material. Generally, speed, 3D printer prices, the printed prototype and the choice and cost of the materials as well as coloring capabilities are key considerations in selecting a computer. Metal printers are typically costly that work directly. However, a mold that is used to manufacture metal parts may be used to produce less costly printers.

ISO / ASTM 52900-15 describes in its importance seven types of AM processes: sheet lamination, powder bed fusion, binder jetting, material jetting, material extrusion, vat photopolymerization, and directed energy deposition [19].

Some techniques melt the material or soften it to create the layers. The model or component is formed by the extrusion of little beads or streams of material that immediately harden to form layers for the manufacturing of fused filament, also known as fused deposition modeling (FDM). Thermal plastic filament, wire of metal or some other material are filled into a nozzle head (3D printer extruder), which heats up and disconnects the material. In the variety of forms that can be produced, FDM is a little limited. Another method fuses sections of the layer, then goes up into the workspace, adds yet another granular layer and repeats the process until the component is made up. This process utilizes unfused media to support overhangs and thin walls of the manufactured component, reducing the need for temporary supports for the product. FFF / FDM has recently been extended directly from the pellets to 3D print to prevent filament conversion. The Fusion Particle Manufacturing (FPF) process is a process that has the ability to use more recycled materials [20].

Multi-process Powder Bed Fusion or PBF involves a range of processes including DMLS, SLS, SLM, MJF and EBM. With a variety of materials, Powder Bed Fusion processes are suitable, and its versatility allows for geometrically complex structures [67] which makes it an option for many 3D printings projects. These include selective laser sintering with metals and polymers and direct laser sintering with metal. Selective laser melting does not use sintering for fusing powder granules but melts the powder entirely with a high-energy laser to produce densely paced materials with a mechanical characteristic close to those used in traditional metals. Electron beam melting is a similar method of metal parts (titanium alloys) manufacturing additive technology. EBM creates the pieces

with a high-vacuum electron beam by layer melting metal powder layer by layer. Another method involves a 3D inkjet printer that produces a one-size-only model, spreading the powder layer (plaster or resins) and pressing the binder via an inkjet process in the cross-section of the component. Thin layers are cut to form and combined with the laminated object output. In addition, HP invented the Multi Jet Fusion (MJF), a Pulver-based technique that is not involved with lasers, alongside the methods described previously. The fusion and detailing agents are added to an inkjet table, then joined to create a solid layer by heating [21].

1.1.4 Application

3D printing or additive manufacturing has been used in manufacturing, medical, business, and sociocultural sectors in the current scenario, promoting the effective commercial technology of 3D printing or additive manufacturing. More recently, 3D printing has also been used to manufacture a variety of medical products, prosthetics, spares and replacements in the humanitarian and development market. The earliest additive manufacturing application was at the end of the output continuum in the toolroom. For example, one of the earliest additive variants was rapid prototyping, and its goal was to minimize the lead time and expense of producing prototypes of new components and products, which was previously achieved only through subtractive tool room techniques such as CNC milling, spinning, and precision grinding. In the 2010s, much more production entered additive manufacturing.

Food AM is being produced by pressing food into three-dimensional objects, layer by layer. A wide range of foods are suitable candidates, such as chocolate and sweets, and NASA is researching the technology for flat foods such as crackers, pasta, and pizza in order to produce 3D printed foods to minimize food waste and to make foods that are tailored to meet the nutritional needs of an astronaut. Italian bioengineer Giuseppe Scionti invented a technology in 2018 to produce fibrous plant-based meat analogs using a custom 3D bioprinter, mimicking meat texture and nutritional values.

AM has a two-dimensional effect on firearms: new processes for the manufacturing of existing firms and new markets for do-it-yourself fire armed guns. In 2012, the US-based Defense Distributed community released plans to develop a working 3D printed weapon, "which can be downloaded and replicated by anyone using a 3d printer," raising questions about the impact of 3D printing and wide specific CNC machining at market level [22] on gun control efficiency [23].

Operational therapies for 3D printing have a tradition of anatomical modeling for bony reconstructive surgery preparation since the mid-1990s. Patient-coordinated implants were a natural extension of this work, resulting in genuinely customized implants that suited a single person. Digital surgical

scheduling and 3D guidance have been applied with great success to many surgical fields, including full articulation substitution, and craniomaxillofacial reconstruction. One such example is the bioresorbable tracheal splint developed at the University of Michigan for the treatment of newborns by tracheobronchomegaly [24]. Also, the use of additive manufacturing for serialized production of orthopedic implants (metals) has increased as porous surface structures can be efficiently produced to promote osseous-integration. The hearing aid and the dental industry should be the largest field of further growth with the personalized 3D printing technology.

1.2. Stainless steel

1.2.1. Introduction

Stainless steel [25] is an iron-based alloy category of at least 11% chromium [26], which prevents iron from rusting,[7], and provides heat-resistant characteristics. The elements of carbon (from 0,03% to above 1,0%), nitrogen, aluminum, silicon, sulfur, titanium, nickel, copper, selenium, niobium and molybdenum are found in various forms of stainless steel. The three-digit number for particular types of stainless steel, e.g. 304 stainless, is also suggested.

The resistance of stainless steel to the formation of ferric oxide results from chromium being present in the alloy which forms a passive film which protects the material against corrosion, and which can heal itself in the presence of oxygen. The resistance to corrosion can be further improved by:

- raising the content of chromium to 11% [27]
- 8 % addition or higher nickel quantities
- Added molybdenum (which also increases "pitting" corrosion resistance).

Adding nitrogen would also improve corrosion resistance and increase mechanical strength. As a result, the alloy is tolerated for the environment in different grades of stainless steel with various material chromium and molybdenum [28].

Corrosion resistance, low maintenance and familial luster make stainless steel suitable for a variety of applications involving both steel strength and corrosion resistance. In addition, in stainless steel sheets, plates and bars, wire and tubing may be rolled. These may be used in cookware, cutlery, operating machines, machinery, construction materials in large buildings, manufacturing equipment (for instance in paper mills, chemical plants, water treatment), storage tanks and tankers for chemical products and food products. The resistance to corrosion of the materials, the simplicity of steam purifying and sterilizing as well as the failure to require surface coating have contributed to the use of stainless steel in kitchens and food processing plants.

1.2.2. Stainless steel families

Five major families are classified mainly by their crystalline structure: ferritic, austenitic, duplex, martensitic, and precipitation hardening.

Austenitic stainless steel [29] is the largest family of stainless steels that account for about 2/3 of all production of stainless steel. They have an austenitic, facially centered cubical crystal structure. They are made by alloying nickel and/or manganese and nitrogen enough to retain an austenitic microstructure at all temperatures from the cryogens to the melting point [30], and this microstructure is accomplished by alloying steel. Austenitic stainless steels are therefore not tough for heat treatment because at all temperatures they have the same microstructure.

In addition, austenitic stainless steels can also be subdivided into 2 groups:

- 200 series consist of chromium-manganese-nickel alloys to reduce the use of manganese and nitrogen. They have approximately 50% more productivity because of the addition of their nitrogen than stainless steel sheets of the 300 series.

  o Type 201 can be hardened by cold work.
  o Type 202 is stainless steel for general purpose. The decrease in nickel content and the rise in manganese lead to poor resistance to corrosion [31].

- 300 series are chromium-nickel alloys, which almost exclusively use nickel alloys to achieve their austenitic microstructure; some very high alloys contain some nitrogen to minimize nickel requirements. The largest and most frequently used group is the 300 series.
  o Type 304: The most well-known class is Type 304, also known as 18/8 and 18/10, for its 18% chromium and 8% 10% nickel composition.
  o Type 316: is the second most common austenitic steel. Adding 2% molybdenum has a higher acid and localized corrosion resistance due to chloride ions. Low-carbon variants like 316L or 304L have less than 0.03 percent carbon content and are used for the prevention of welding corrosion [32], [33].

Ferritic stainless steels have a ferrite, body-centered, microstructural microstructure, such as carbon steel, which contains between 10.5% and 27% chromium, with very little to no nickel. This microstructure is present at all temperatures due to the addition of chromium and is not thermal hardy. Cold work cannot strengthen them to the same extent as austenitic stainless steels. They are magnet. They are magnetism.

Since nickel is almost absent, it is cheaper than austenitic steels and is present in many products, including:

- Car exhaust pipes (Type 409 and 409 Cb are used in North America; Type 439 and 441 are used in Europe in stabilized grades).
- Architectural and structural (type 430 comprising 17% Cr) applications.)
- Building components, such as slate hooks, roofing, and chimney ducts.
- Solid oxide fuel cell power plates oscine nickel is almost absent, it is cheaper than austenitic steels and is present in many items including temperatures around 700 ° C (1,292 ° F) (high chromium ferritic containing 22 percent Cr) [33].

Martensitic stainless steels are used as stainless engineering steels, stainless steel tool steels, and creep-resistant steels and provide a wide variety of properties. Due to their low chromium content, they are magnetic, and not as corrosion resistant as ferritic and austenitic stainless steels. They fall (with some overlap) into four groups.:

1. Cr-C grades: These were the first grades used in engineering and wear-resistant applications and are still commonly used.
2. Grades of Fe-Cr-Ni-C: Some carbon is substituted with nickel. They deliver greater durability and greater resistance to corrosion. For most Pelton, Kaplan, and Francis turbines in hydroelectric power plants, grade EN 1.4303 (Casting grade CA6NM) with 13 percent Cr and 4 percent Ni is used [34] because it has good casting properties, good weldability, and good cavitation erosion resistance.
3. Grades of precipitation hardening: Grade EN 1.4542 (also known as 17/4PH), the best-known grade, blends martensitic hardening and hardening of precipitation. This achieves high strength and strong durability and is used among other applications in aerospace.
4. Creep-resistant grades: Small vanadium, niobium, boron and cobalt additions improve strength and resistance to creep up to around 650 ° C (1,202 ° F).

To have better mechanical properties, martensitic stainless steels can be thermally treated.

Usually, heat treatment requires three phases:

1. Austenitizing, depending on grade, in which the steel is heated to a temperature in the range of 980-1,050 ° C (1,800-1,920 ° F). The resulting austenite has a cubic crystal face-centered composition.

2. Quenching: Martensite, a hard body-centered tetragonal crystal structure, is converted into austenite. For most uses, the quenched martensite is very tough and too brittle. There may be some residual austenite remaining.

3. Tempering: The martensite is heated to a temperature of approximately 500 ° C (932 ° F), then air-cooled. Higher temperatures reduce yield strength and ultimate tensile strength but increase elongation and resistance to impact.

It is a recent trend to substitute some carbon in martensitic stainless steels with nitrogen. The limited solubility of nitrogen is improved by the Pressure Electroslag Refining (PESR) process, in which high nitrogen pressure melting is carried out. Up to 0.4 percent nitrogen containing steel has been achieved, resulting in higher hardness and strength and higher corrosion resistance. Since PESR is costly, the standard argon oxygen decarburization (AOD) process has been used to achieve lower but important nitrogen levels [35].

Duplex stainless steels have a mixed austenite and ferrite microstructure, with a 50:50 mix being the optimal ratio, whereas commercial alloys could have 40:60. Higher chromium (19-32 percent) and molybdenum (up to 5 percent) and lower nickel content than austenitic stainless steels describe them. **Duplex stainless steel** has a yield strength of approximately twice that of austenitic stainless steel. Compared to austenitic stainless steel types 304 and 316, their mixed microstructure provides better resistance to chloride stress corrosion cracking.

Based on their corrosion resistance, duplex grades are commonly classified into three sub-groups: lean duplex, regular duplex, and super duplex.

With an overall lower alloy content than similar-performing super-austenitic types, the properties of duplex stainless steels are achieved, making their use cost-effective for many applications. One of the first to utilize duplex stainless steel widely was the pulp and paper industry. The oil and gas industry are the largest consumer today and has lobbied for more grades that are resistant to corrosion, contributing to the growth of super duplex and hyper duplex grades. More recently, the less costly (and slightly less corrosion-resistant) lean duplex has been developed, primarily for building and construction structural applications (concrete reinforcing bars, bridge plates, coastal works) and in the water industry.

Precipitation hardening stainless steels have similar corrosion resistance to austenitic varieties but can harden to even higher strengths than other martensitic grades for precipitation hardening. There are three types of stainless steel precipitation hardening:

- AISI 630 EN 1.4542 (Martensitic 17-4 PH) comprises around 17 percent Cr, 4 percent Ni, 4 percent Cu, and 0.3 percent Nb. Solution treatment at about 1,040 ° C (1,900 ° F) accompanied by quenching results in a martensitic structure that is relatively ductile. Subsequent aging treatment at 475 ° C (887 ° F) precipitates phases rich in Nb and Cu that increase the yield intensity up to over 1000 MPa. In high-tech applications such as aerospace (usually after remelting to remove non-metallic inclusions, which improves the fatigue life), this outstanding strength level is used. Another big benefit of this steel is that, unlike tempering procedures, aging is carried out at a temperature that can be applied without distortion and discoloration to (nearly) finished sections.

- A semi-austenitic 17-7PH (AISI 631 EN 1.4568) comprises approximately 17% Cr, 7.2% Ni, and 1.2% Al. Typical heat treatment requires treatment of solutions and quenching. At this point, the structure stays austenitic. Martensitic conversion is then accomplished either by cryogenic treatment at -75 ° C (-103 ° F) or by extreme cold work (over 70 percent deformation, normally through cold rolling or wire drawing). Aging on almost finished components at 510 ° C (950 ° F), which precipitates the intermetallic process of Ni3Al, is carried out as above. The level of yield stress is then reached above 1400 MPa.

- Austenitic A286 (ASTM 660 EN 1.4980) comprises approximately 15% Cr Ni 25%, Ti 2.1% Mo 1.2%, V 1.3%, and B 0.005%. For all temperatures, the structure remains austenitic. Typical thermal treatment consists of treatment and quenching of solution, followed by 715 ° C (1.319 ° F) ageing. Aging Ni3Ti precipitates and increases the potential of the yield at room temperature to about 650 MPa. Contrary to the above, this stainless steel remains very strong mechanical properties and crept resistance at temperatures up to 700 ° C. A286 is therefore known as a Fe-based superalloy for jet motor, gas turbines and turbo components.

1.2.3. Properties

2. Unlike carbon steel, in wet conditions, stainless steels suffer from uniform corrosion. Unprotected carbon steel is quickly rusted when exposed to air and humidity. It creates a porous and fragile layer of iron oxide. In addition, as this layer extends and continues to flow and fall by taking iron oxide in a greater volume than the initial steel, the underlying steel is subjected to further attacks. In contrast, stainless steels produce enough chromium to passive forming, by reaction to oxygen in the air and the little amount of dissolved oxygen in the water, micro sculpturally thin inert

surface layer of chrome oxide. This passive film prevents further corrosion, prevents the spray of oxygen from spreading to the steel surface [36]. This film is naturally self-reparative even if the disruption of an atmosphere is scratched or temporarily disrupted, which exceeds this grade's corrosion resistance [37].

3. The corrosion resistance of this product depends on the chemistry of the stainless steel, particularly the content of chromium. The four modes of corrosion are generally distinguished: uniform, localized (pitting), galvanic and SCC (stress cracking). Any such corrosion type can occur if the stainless steel grade is not suitable for work.

4. The word "CRES" refers to steel that is resistant to corrosion. CRES refers most, but not all, to stainless steel, which can also be corrosion resistant to non-stainless steel materials [38].

5. Like steel, stainless steels are relatively weak electricity conductors, with even less conductivity than copper. The thick protective oxide layer of electrical contact resistance of stainless steel (ECR) in particular, restricts its usefulness as an electrical connector in applications. The lower ECR values and the chosen materials for such applications are cotton alloys and Nickel-coated connectors. In cases where ECR is less engineered and less corrosion resilient, e. g. in high temperatures and oxidizing conditions, stainless steel connectors are used.

1.2.4. Application

The use of steel can be functional and esthetic in houses. Mainly known in the Art Deco era, the upper section of the Chrysler building demonstrates the most famous use of stainless steel. Many of these buildings preserved their original appearance due to their longevity.

The buildings of modern buildings, such as the outside of the Twin Towers of Petronas and the Jin Mao building, are designed using infinite steel [39]. The Australian Parliament House in Canberra features 220 tons (240 short tons) stainless steel flagpole. The aeration building at Edmonton Composting Facility is the largest stainless steel structure in North America. La Geode in Paris consists of 6433 polished equilateral triangles of stainless steel that make up the sphere that represents the sky. The production of high-strength grades of stainless steel, including "lean duplex," led to increased use in structural applications.

Owing to its low reflectivity, stainless steel is used as an airport roofing material that prevents pilots from blinding. It is often used to maintain the roof surface warm to the ambient temperature. Examples include the International Airport Sacramento in California and the International Airport Hamad in Qatar.

In the shape of tubes, pipes, or strengthening bars, the stainless steel is used for pedestrian and road bridges. Examples are the first stainless steel road bridge to be erected on the Cala Galdaña Bridge in Menorca, the Champlain Bridge in Montreal [40], the Amsterdam Oudesluijs Bridge, which was created from Construction 3D printing; the Bilbao Padre Arrupe Bridge, which connects the University of Deusto to the Bilbao Museum of Guggenheim [40]. Spain's Sant Fruitos Footbridge; Hong Kong's Stones bridge; Singapore's Helix Bridge. Footbridge.

CHAPTER 2 – EXPERIMENTAL PROCEDURES

5.1. 2.1. Powder bed fusion

5.2. 2.1.1. Introduction

The process of Powder Bed Fusion involves the following common printing techniques: Electron beam melting (EBM), Direct metal laser sintering (DMLS), Selective heat sintering (SHS), Selective laser sintering (SLS) and Selective laser melting (SLM).

Methods of Powder bed Fusion (PBF) are to melt powder together with laser or electron beam. Electron beam melting (EBM), procedures require vacuum but can be used in the development of usable components with metals and alloys. The distribution of powder over previous layers is a function of all PBF processes. This is possible by various mechanisms, including a roller or a brush. Fresh material is supplied by a hopper or a tank below the bed. DMLS is the same as SLS, but is used for metals, not plastics. Powder is sintered layer by layer in the process. The use of a heated thermal printer head to fuse the powder content in combination is selective heat sintering. As previously, layers are added with a roller between layer fusion. The model is lowered by a platform.

The PBF process consists of the following steps:

1.   A 0.1 mm thick coating is spread around the building platform.

2.   The first layer or first cross section of the model fuses with a laser.

3.   A new powder layer is distributed in a roller over the previous layer.

4.   Additional layers or cross sections are combined and inserted.

5.   The process continues until the whole model is established. Loose, unfused powder is still in place but extracted after processing.

5.3. 2.1.2. Selective laser melting

Selective laser melting (SLM) is a rapid prototyping, 3D printing, or additive manufacturing (AM) technology, also called direct metallic laser melting (DMLM) or Laser Powder bed Fusion (LPBF), which uses high power laser densities to melt and fuse metal powders together [42][43]. SLM is known by many subcategories as a selective laser sintering (SLS). The SLM process will melt the

metal content in its entirety into a three-dimensional solid component in comparison to SLS.

SLM uses several alloys that allow prototypes to operate as hardware made of the same material as components for production. Since these components are made layer by layer, organic geometries, internal features and difficult passages can be crafted which cannot be casted and machined in any other way. SLM produces solid, robust metal components, both functional prototypes and production components [44].

The method begins by splitting the 3D CAD file data between 20micron and 100micron files into layers, producing 2D images on each layer; this file format is the industry-standard file. This file is then loaded into a program for file preparation that assigns parameters, values and support for the interpretation and construction of the file on various types of additive manufacturing machines.

Thin layers of atomized metal powder are uniformly distributed with selective laser melting on a substratum plate, normally metal, with a cover mechanism connected to an indexing table traveling on the vertical (Z) axis. This occurs inside a chamber with an inert gas, argon or nitrogen tightly regulated atmosphere at levels of oxygen below 500 parts per million. Each 2D part of a geometry part can be fused by melting selectively the powder until each layer has been spread. This is done with a high-performance laser beam, normally a hundred watts ytterbium fiber laser. With two high-frequency scan mirrors, the laser beam is directed in X and Y directions. Laser energy is sufficiently intense to allow the particles completely to melt (sweat) into solid metal. The method is repeated layer by layer until the component is done.

A 200- watt Yb-fiber optical laser is used in the SLM machine. There are a material dispensing platform and a building platform inside the construction chamber, along with a recycling blade for pushing fresh powder over the platform. Metal powder is melted locally using the directed laser beam by the technology. The components are constructed layer by layer, typically 20 micrometer thick layers. [45].

Complex geometry and structures with thin walls and secret gap or canals, on the other hand or with low lot sizes, are the most appropriate types of applications for the Selective Laser Melting technique. Advantage can be obtained by creating hybrid shapes that can be created together by producing solid, partially shaped or lattice geometries to create one single object, such as a hip stem, acetabular bowl, or other orthopedic implant where surface geometry improves osteointegration. A large part of the groundbreaking activities with selective laser melting technologies are on aerospace lightweight parts [46] in which conventional manufacturing constraints, such as equipment and physical access to machining surfaces, limit component design. Instead of eliminating waste material, SLM allows

components to additionally form near the net forming components.

A relatively large amount of set-up (e.g. for mold creation) is costly for conventional methods. Although SLM costs a large amount (mostly because it takes time), it is recommended that only a few parts be produced. This refers, for example, to replacement parts of old machines or to specific goods such as implants (e.g. antique cars).

Tests by the NASA Marshall Space Flight Center, where tests were carried out with the technique of making nickel alloy parts difficult to produce for rocket engines J-2X and RS-25, show that technically difficult components are a little weaker than forged and milled parts. [47].

This technology is used to produce direct components for a wide range of industries, among them small and medium-sized aerospace, dentistry, medical and other industries, highly complex components, and tooling for direct tooling inserts. DMLS reflects a technology that is both cost efficient and time efficient. The technology is used to quickly test new products as it reduces production time and manufacturing as an inexpensive tool for simplifying assemblies and complex geometries [48].

In this study, printed parts were fabricated by Metalsys 120D PBF machine supplied by Wiforsys Co., Ltd (Korea) (Figure 2).

Figure 2. metalsys 120D PBF machine

5.4. 2.2. Material

Stainless steel 316L is a type of molybdenum bearing austenitic stainless steel. It is more resistant to general corrosion and pitting in stainless steels such as 302-304 than conventional nickel chromium. It provides the following features:

- Higher creep resistance

- Corrosion and pitting resistance.

- High temperature rupture and tensile strength

- Excellent formability

Shapes differ according to the type of industrial application, for example: the cookware, cutlery, hardware, operating instruments, major machinery, industrial equipment and construction materials for skyscraper and large buildings. The shapes vary by type of industrial applications.

5.5. 2.3. Heat treatment

Heat treatment (or heat treating) is a range of industrial, hot and metalworking methods used to change the physical properties of a material, and chemical properties. Metallurgical is the typical application. In manufacturing many other materials, including glass, heat treatments are also applied. Heat treatment includes the use, typically at high temperatures, of heating or cooling to produce the wanted result, for example the hardening or softening of a substance. Heat treatment strategies include rectifying, hardening cases, strengthening precipitation, enticing, carburizing, standardizing, and squeezing. While heat treatment refers only to processes where heat and cooling are carried out purposely for the purpose of changing property, heating and cooling are also by chance during other processes such as heat forming or welding.

5.6. 2.4. Characterization analyses

2.4.1 X-ray diffraction (XRD)

X-ray diffraction in materials science is a very effective instrument. This technology is flexible to distinguish phases of a sample. Metals have basic crystal structures and hence fewer peaks in the pattern of diffraction. Crystals are standard atomic arrays and electromagnetic radiation waves may be considered as X-rays. Atoms disperse X-ray rays, mostly by the electrons of the atoms. Much as an ocean wave entering a lighthouse causes secondary circular waves from the lighthouse, so even an X-ray hitting an electron induces secondary spherical waves from the electron. This is called elastic dispersion, and the electron (or light) is known as the dispersion. A standard range of spherical waves are generated by a regular test. Although these waves cancel one another by destructive interference

in most directions, they add in a few concrete directions, defined by Bragg law:

$$2d \sin\theta = n\,\lambda$$

Where: - d is the spacing between diffracting planes,

   - θ is the any integer

   - λ is the wavelength of the beam.

These instructions are called reflections as sports on the diffraction pattern. The X-ray diffraction results therefore from an electromagnetic wave (x-ray) that impacts on a normal range of differences (the repeating atoms in the crystal).

2.4.2 Optical microscope, SEM analyses

The optical microscope, which is also called a light microscope, is a type of microscope which generates magnified images of smaller objects typically by using visible light and a lens device. The oldest microscopic design is optical microscopy, which in 17th century was perhaps invented in their current form. Basic optical microscopes can be very simple, although many advanced designs are intended to improve sample contrast and resolution.

The object is positioned on a stage and can be seen on the microscope directly through one or two oculars. Usually, all ore pieces display the same image in high-power microscopes, but a stereo microscope is used to generate a 3-D effect with slightly different images. The picture is normally captured by a camera (micrograph).

In different ways, the sample can be illuminated. Transparent objects can light from underneath and solid objects may be illuminated by light (bright field) or by the objective lens (dark field). The crystal-orientation of metallic objects can be determined by Polarised light. Phased imagery can be

Figure 3. Olympus BX51M metallurgical microscopy

used to improve the contrast of the image by stressing small details of the different refractive index.

The microstructure of printed specimens was observed and analyzed by Olympus BX51M optical microcopy (Figure 3) in this study.

Scanning electron microscope (SEM) is a type of electron microscope that generates sample pictures using a focused electron beam to scan the region. The electrons interact with atoms in the sample and produce different signaling data on the surface topography and sample composition. The beam is scanned in a raster scan pattern, and the beam position is combined with the signal intensity for an image. In the commonest SEM mode, the Everhart-Thornley sensors detect secondary electrons emitted from atoms excited by the electron beam. Among other things, depends on specimen topography. The number of secondary electrons that can be detected and hence signal strength. Some SEMs can generate more than 1 nanometer resolution.

2.4.3 Porosity and hardness measurement

Porosity or void fragment is a measure of the empty space in a substance that is a fraction of the total volume of voids between 0 and 1, or between 0 and 100%. Strictly speaking, some tests calculate the "open distance," the total surface area accessible.

A material or component may use several different tests for porosity, such as industrial CT scanning. The word 'porosity' is employed in numerous fields, including pharmaceuticals, ceramics, metallurgy, materials, hydrology, soil engineering, and hydrology.

In this work, the porosity of printed samples was calculated by OM image through ImageJ software.

Figure 4. logo of image J software [52]

Hardness is a resistance test of plastic localized deformation caused by mechanical indentation or abrasion, respectively. Certain materials (for example, metals) are tougher than other goods (for example, plastics, wood). In general, macroscopic hardness is characterized by high intermolecular bonds, but the action of solids under force is complex; thus, the different hardness measurements exist hardness scratch, hardness in the indentation and hardness rebound. Durability is based on ductility, rigidity, plasticity, strain, strength, strength, viscoelasticity, and viscosity. Popular examples of hard material are pottery, concrete, some metals, and super hard materials that can be compared to soft materials.

Vickers Hardness tester (Figure5) supplied by Mitutoyo Co., Ltd (Japan) was performing in to prove more data to relate to the strength of the initial samples in this study.

Figure 5. Mitutoyo Vickers Hardness tester MVK-H1

2.4.4 Tensile test

Tensile strength means measuring the force to pull something like a rope, a wire or a structural beam so that it breaks out.

The tensile strength of a material is the highest tensile stress it can take before failure.

The tensile strength definitions are three typical definitions:

- Yield strength - Without continuous deformation the stress of a material will stand out. This is not an established problem sharply. The yield strength is the stress that causes the original dimension to permanently deform 0,2%.

- Ultimate strength - The highest stress that a material can withstand.

- Breaking strength - The stress co-ordinates on the stress curve at the rupture point.

Tensile tests are a basic materials science and engineering test in which a sample is subjected to controlled stress up to failure and known as tension tests [49]. The properties that are evaluated directly via a tensile test are ultimate strength, breaking strength, maximum length, and surface reduction [50]. The following characteristics can also be calculated from these measurements: Young Module, Poisson ratio, yield point, and stress hardens [51]. The most popular application for mechanical properties of isotopically materials is uniaxial tensile research. Some products are tested with biaxial tensile. How load is applied to the materials is the key difference between this test machine.

Tensile testing can have several goals:

- Pick an application material or object.

- Forecast the use of material: natural and extreme forces.

- Assess if the specifications, rules or contracts conditions are fulfilled or reviewed.

- Determine if a new product development program is being introduced.

- Prove principle proof.

- Show the usefulness of the proposed patent.

- Provide uniform data for other roles of research, technological and quality assurance.

- Set the groundwork for professional contact.

- Have a technical way to compare different options.

- Furnish proof in legal proceedings.

A universal testing machine (Figure 6) was used for this test.

Figure 6. Universal testing machine

CHAPTER 3 – INVESTIGATION OF EFFECTS OF PROCESS PARAMETERS ON MICROSTUCTURE AND PROPERTIES OF 316L STAINLESS STEEL PRODUCED BY ADDITIVE MANUFACTURING PROCESS

5.7.3.1. Introduction

Powder bed fusion (PBF) is an additive manufacturing (AM) process whereby layers of powdered plastic or metal are melted by a laser or electron beam to create three-dimensional (3D) objects. 316L stainless steel, which has low carbon content creating welding ability to avoid carbide precipitation, is appropriately selected in this work. In this present study, 3D objects of 316L stainless steel are manufactured from powder by PBF with different experimental conditions. The laser power affects the amount of energy applied to melt the powder layer and to create an active melting pool. The goal of this study is to investigate the relationship between mechanical and material properties of printed 316L stainless steel samples and different laser power parameter of 144 W and 180 W in PBF. The microstructure analyses of printed samples are investigated by optical microscopy (OM), scanning element microscopy (SEM) to evaluate the effect of laser power parameter in PBF. The hardness of printed samples is then also measured by Vickers hardness indenter.

5.8.3.2. Experimental procedure

3.2.1. Material

The material used in this study was 316L stainless steel powder supplied by Orelikon Metco (US). The powder diameter was a range from 15 µm to 45 µm. Figure 7 showed that morphology of the 316L stainless steel powder was spherical. The microstructure of the cross-section of initial 316L stainless steel powder was showed by optical microscopy (OM) in Figure 8. The X-ray diffraction (XRD) phase patter and energy-dispersive X-ray spectroscopy (EDS) image of 316L stainless steel
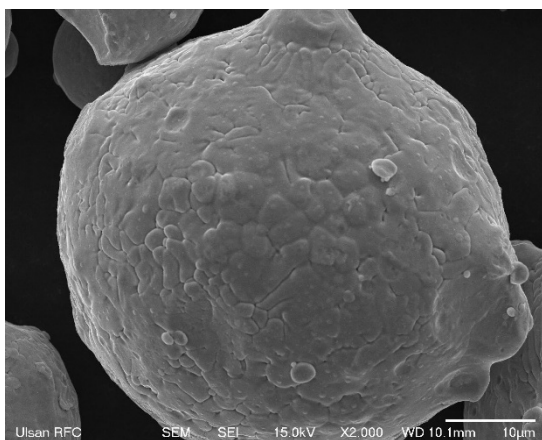

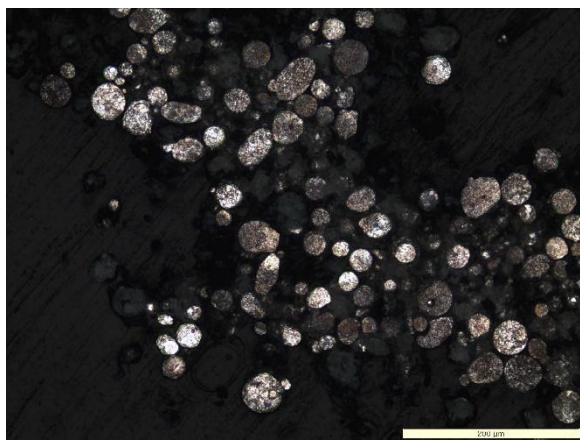Figure 7. SEM image of 316L stainless steel powder

Figure 8. OM image of 316 stainless steel powder

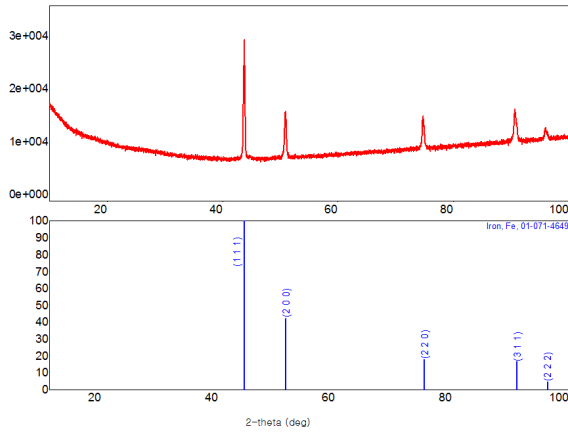powder were presented in figure 10 and figure 9, respectively.

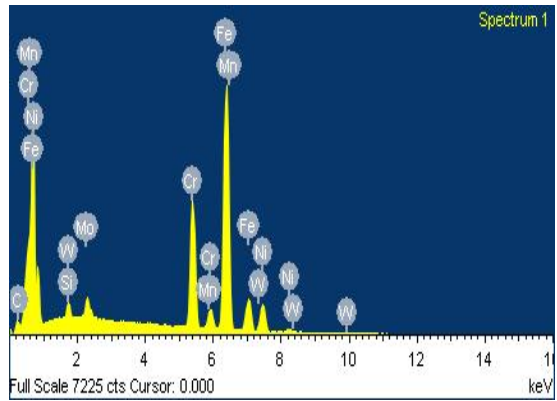Figure 10. XRD phase pattern of 316L stainless steel powder

Figure 9. EDS image of 316L stainless steel powder.

Figure 11. Image of 316L stainless steel sample after printing
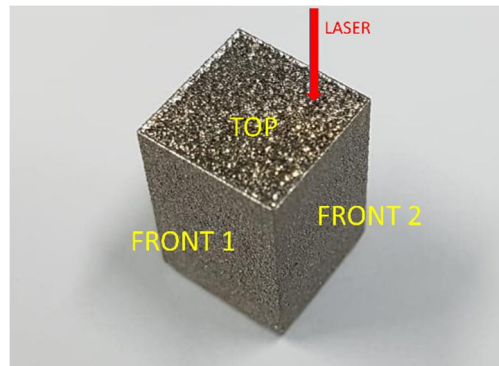
1.2.2   Sample manufacturing

316L stainless steel samples were manufactured by Metalsys 120D PBF machine provided by Winforsys Co., Ltd (Korea). The dimension of samples was 10x10x15 mm as shown in figure 11. The experimental design for this study was divided into two parts denoted by A and B. The printed parameters of printed parts were listed in Table 1.

Table 1. Specimen classification by process conditions

	Laser speed (mm/s)	Laser power (W)	Sample size
Sample A	750	180	10x10x15
Sample B	750	140	10x10x15

3.2.3. Analytical methods

The printed parts were observed by conventional procedures. The samples were grinded with seven different grades of sandpaper (#400, #600, #800, #1000, #1200, #1500, #2000) and polished down to 1 μm. And then, the samples were etched and observed surface using optical microscopy (OM). microstructure surface of samples was observed on all three sides of samples as shown figure

Vickers hardness test provided by Mitutoyo Co., Ltd (Japan) was effectuated to collect data relate mechanical property of samples. Each sample was measured five times with the setting load of 980.665 mN to get more accurate results.

5.9.3.3. Results and discussion

3.3.1 Hardness

The average hardness at each sides of printed parts was presented in Table 2. As the results, the average hardness of samples was different among sides. The hardness of top view was higher than that of front view in both samples. And, the hardness of sample B was higher than that of sample A for all sides.

Table 2. The hardness of 316L Stainless steel samples

	Hardness (HV)		
	Top	Front 1	Front 2
Sample A	212 ± 5	208 ± 6	206 ± 9
Sample B	219 ± 4	213 ± 8	210 ± 5

3.3.2 Sample microstructure

3.3.2.1. Top view

Microstructure at top view of samples was observed by optical microscopy (OM) as shown in Figure 12. For sample A, there were many defects which appear during printing such as non-melting areas

and pores. Many irregular pores with size from 10 µm to 100 µm were formed in certain way inside in
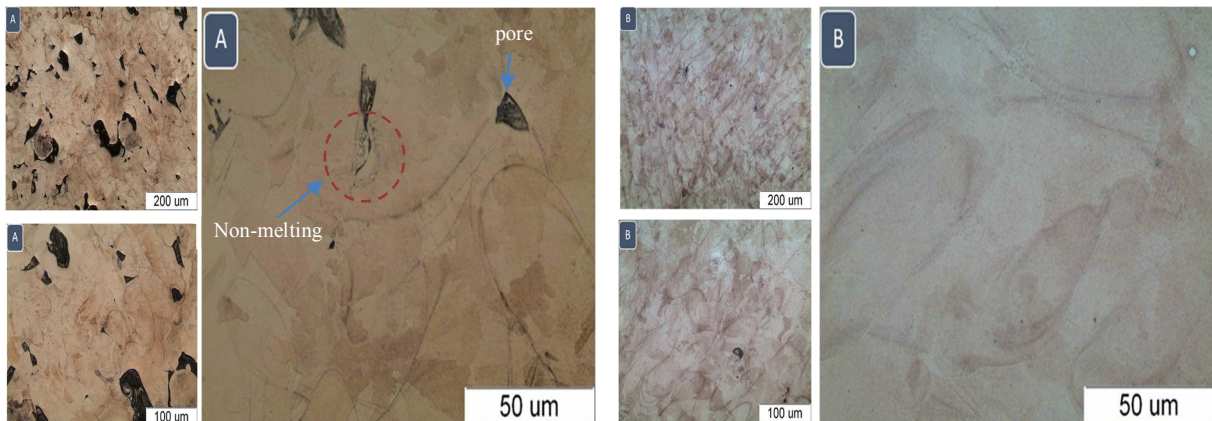

Figure 12. OM image of top view of printed samples

the sample. For sample B, the defects appeared insignificantly. The size of pores in samples B was smaller than that in samples A. Non-melting areas did not appear inside the sample B. the melt pools were elliptically shaped profile and these melt pool overlapped in a specific arrangement.

3.3.2.2. Front view

Figure 13 and figure 14 showed the microstructure at front views of printed samples. From the results, we can observe that the defects appeared with high density in surface of sample A. The porosity percentage of sample A was 3.42%. The pores were formed with large sized (form 30 µm to 120 µm). The small pores were abundant inside the melting pools. The melting pools were not uniform in sample B.

For sample B, the pores almost were not appeared with porosity percentage of sample just was 0.19%. The melting pools were formed in specific arrangement.
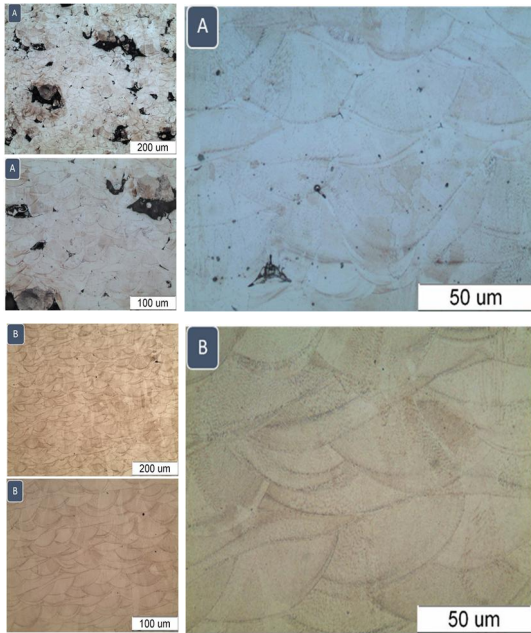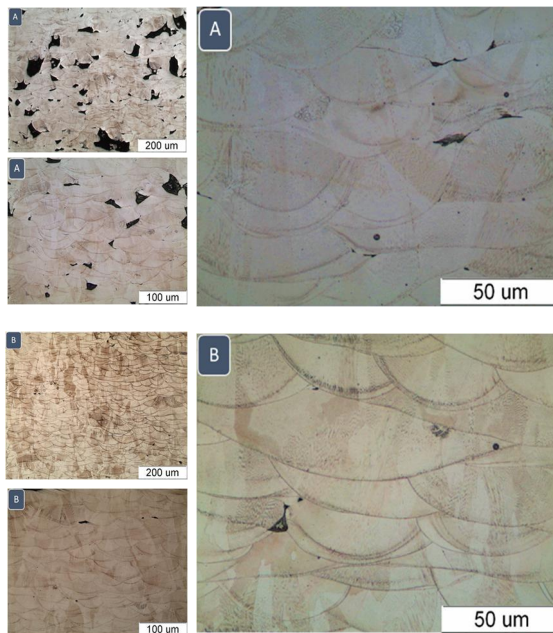
Figure 13. OM image of front view 1 of samples

Figure 14. OM image of front view 2 of samples

3.4. Conclusions

This work concerns the relationship between material properties of printed 316l stainless steel parts and laser power parameters. The laser power of 180W and 144W was used to produce samples with size 10x10x15mm. There are mainly two conclusion that can draw from this work:

- The average hardness of printed samples with laser power of 144W was higher than that with laser power of 180W.
- OM results were confirmed that the printed samples with laser power of 180W had many defects and the melt pools was not homogeneous. Meanwhile, the printed samples with laser power of 144w showed much fewer defects.

According to these results, the suitable laser power of 144W and laser speed of 750 mm/s show promising characteristic and properties of printing 316L stainless steel.

CHAPTER 4 – HEAT TREATMENT AND MECHANICAL PROPERTIES OF 316L STAINLESS STEEL PRODUCE BY ADDITIVE MANUFACTURING PROCESS

5.10. 4.1. Introduction

Powder bed fusion (PBF) of additive manufacturing (AM) is a developing technique to produce complex geometry parts for structural application in aircraft and automotive industries, etc. In the present study, 3D objects are manufactured with 316L stainless steel powder by PBF with different printing orientations. The 316L stainless steel is selected in this work because of its high mechanical strength and excellent corrosion resistant properties. The purpose of this work is to investigate the effect of different printing orientations (X-direction and Z-direction) on the structure and mechanical properties of the manufactured 3D objects after heat treatment. The samples were heat-treated for 2 hours at 650 °C, 950ºC and annealed in the furnace. In the results, tensile test and Vickers hardness test were used to analysis the mechanical properties. The microstructure of the initial powder and the manufactured 3D objects were analyzed by the scanning electron-microscopy (SEM), optical microscopy (OM), etc.

5.11. 4.2. Experimental design

4.2.1. Material

The gas atomized 316L stainless steel powder used in this study was provided by Oerlikon Metco (US). The chemical composition of the 316L powder included Ni, Cr, Mo, Si, Mn, C and Fe is listed in Table 3. Morphology of almost of the 316L stainless steel powder is spherical as shown by scanning electron microscopy (SEM) in Figure 16. The powder diameter is a range from 15 μm to 45 μm. Figure 15 show microstructure of the cross-sections of initial 316L stainless steel powder with Optical microscopy (OM).

The density of the material is indicated in Table 4. The apparent density ($D_{app)}$) and tap density ($D_{tap)}$) of material are 4.49 g/cm^3 and 4.68 g/cm^3, respectively. With Hausner ratio (D_{tap} / D_{app}) [53], [54] is 1.04, the 316L stainless steel is suitable for 3D printing (standard range Hausner ratio from 1.0 to 1.25) [55], [56].

Table 3. Chemical composition of 316L stainless steel powder

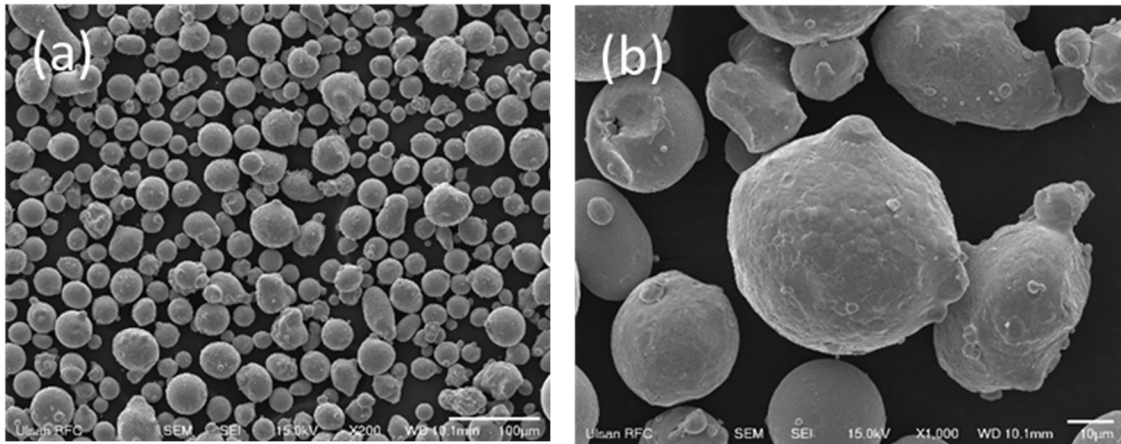| Elements	Fe	Ni	Cr	Mo	Si	Mn	C
Chemical composition (W%)	Balance	12.00	17.00	2.50	2.30	1.00	0.03

Figure 16. SEM image of 316l stainless steel powder. (a) low magnification, (b) high magnification
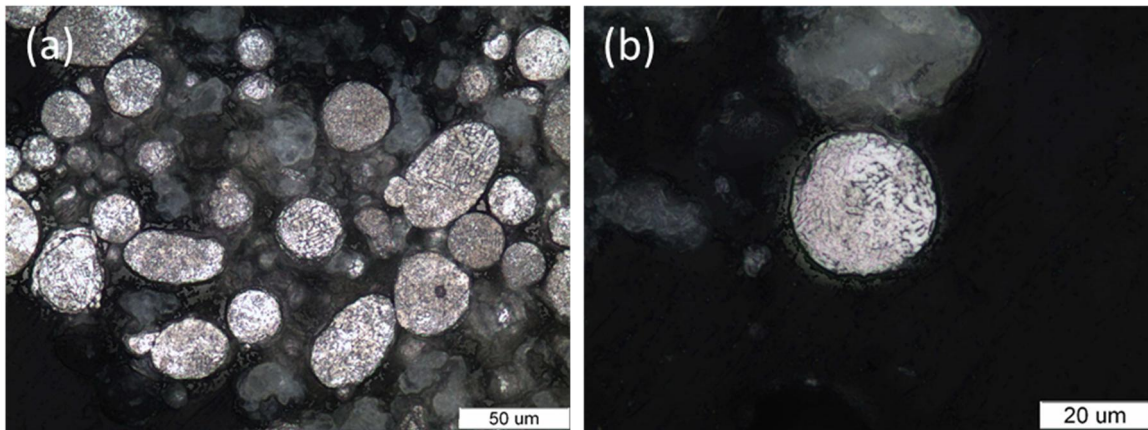

Figure 15. OM image of the 316L stainless steel powder. (a) low magnification, (b) high magnification

Table 4. Characterization of 316L stainless steel powder

Apparent density (D_{app})	4.49 g/cm^3
Tap density (D_{tap})	4.68 g/cm^3
Hausner ratio (D_{tap} / D_{app})	1.04

4.2.2. Sample fabrication

Samples were manufactured by Metalsys 120D PBF machine provided by Winforsys Co., Ltd (Korea). The experimental design for this study was divided into three parts. One part was the block shape with diameter 10x10x10 mm as shown in Figure 18 (a). The other two parts were designed for tensile test as per ISO 22647 standard. The tensile sample was built in horizontal orientation (X-direction) as shown in Figure 18(b), the other tensile sample was built in vertical orientation (Z-direction) as shown

in Figure 18(c). The dimension of tensile samples was described in Figure 17.

The PBF machine parameters used to manufacture those parts were kept unchanged throughout the entire process. The laser power for printing was 144 W, the laser scanning speed was 750 mm/s, and the laser diameter was 0.08 mm.
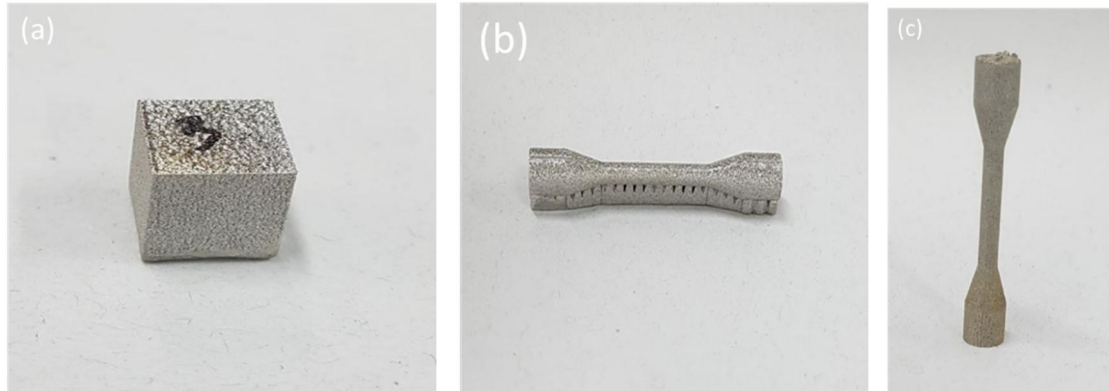
Figure 18. Image of printed samples. (a) block sample, (b) X-direction tensile sample, (c) Z-direction tensile sample
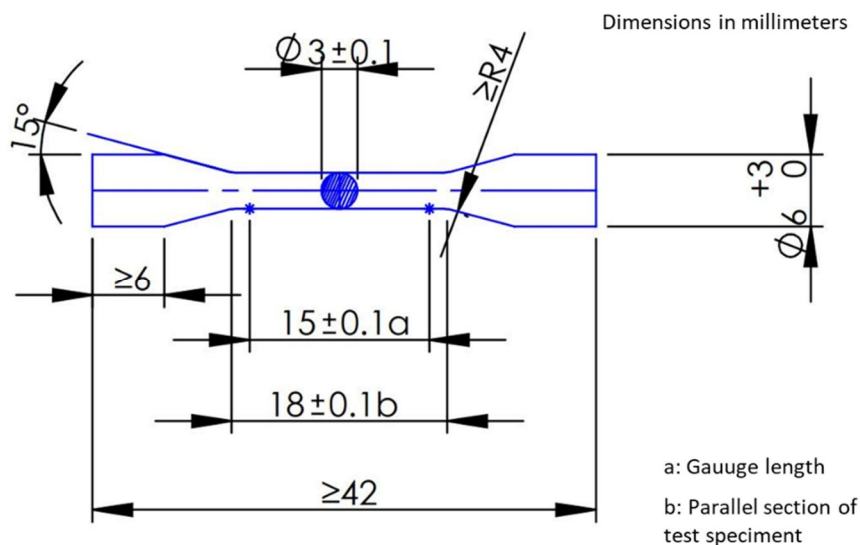

Figure 17. Dimension of tensile test samples (ISO 22647)

4.2.3. Heat treatment

The block samples were assigned to two different heat treatments: low temperature annealing (HT1), high temperature annealing (HT2).

The tensile samples were also assigned to different heat treatments. With horizontal-build samples,

low temperature annealing was as X-HT1, high temperature annealing was as X-HT2. With vertical-build samples, low temperature annealing was as Z-HT1, high temperature annealing was as Z-HT2.

X-HT1 and Z-HT1 were annealed at 650ºC for 2 hours and cooling slowly in the chamber. X-HT2 and Z-HT2 were annealed at 950ºC for 2 hours and cooling slowly in the chamber. The reason for applying 650ºC /2 hours and 950ºC/2 hours of annealing was based on Kamariaha, et al realized that there were changes in the microstructure and mechanical properties of AM samples [57].

4.2.4 Microstructure analysis

The microstructure of printed and the heat-treated parts were observed by conventional procedures. The block sample were grinded with seven different grades of sandpaper (#400, #600, #800, #1000, #1200, #1500, #2000) and polished down to 1μm. Optical microscope (OM) was used to observe the surface of samples. The porosity of samples was calculated by OM image through ImageJ software developed by the National Institutes of Health and the Laboratory for Optical and Computational Instrumentation (LOCI, University of Wisconsin) [58], [59]. After tensile testing, the fracture surface of samples was observed through scanning electron microscope (SEM).

4.2.5. Mechanical test

The tensile test was conducted with the as-built and heat treated samples to collect data to compare with each other. A universal testing machine was used for this test. The strain rate during tensile was 1mm/min in all of samples because the heat treatment samples were expected to have high ductility. Mechanical properties and performance of samples were measured. An extensometer was also used to expressly compute the strain in the samples.

Vickers Hardness tester supplied by Mitutoyo Co., Ltd (Japan) was performing in to prove more data to relate to the strength of the initial samples. Each sample was measured five times to get more accurate results.

5.12.   4.3. Result and discussion

4.3.1. Microstructure

The porosity of the printed samples was determined through ImageJ measurements. OM images were transformed into Image J software and total percentage of black dots corresponding to voids was figure. To remove the risk of variating the pores' concentration effects in different samples parts, the low magnification was used. Five OM images of the polished cross-sections cuts without etching were taken for each sample. The Figure 19 shown the surface cut images of samples. The average porosity was calculated and listed in Table 5.
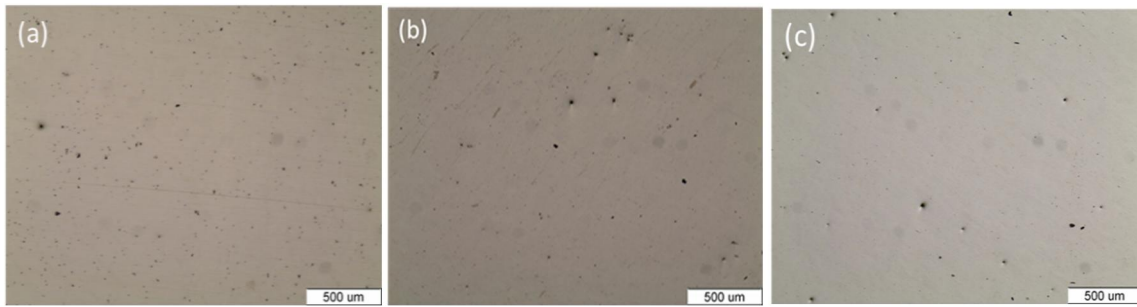
Figure 19. Macro-pore distribution of STS 316L block samples. (a) As-built, (b) HT1, (c) HT2

Table 5. The percentage of block samples

sample	Porosity percentage (%)
As-built	0.11
HT1	0.17
HT2	0.12

The porosity level is almost the same in all of samples. This means that there was a formation of pores during the stage of material fabrication process with as-build condition and no pores were created during heat treatment stage.

Metallographic images of the as-built and heat treated block samples were shown in Figure 20. The elongated powder boundaries and welding boundaries were clearly observed at as-built samples. In the HT1 samples showed there was no internal rearrangement of the material structure during heat treatment at 650°C for 2 hours. However, the powder structures and welding structures completely disappeared in HT2 samples. Instead, we observed the appearance of new grain boundaries. This proved that the recrystallization occurred in the printed sampled during heat treatment at 950°C.
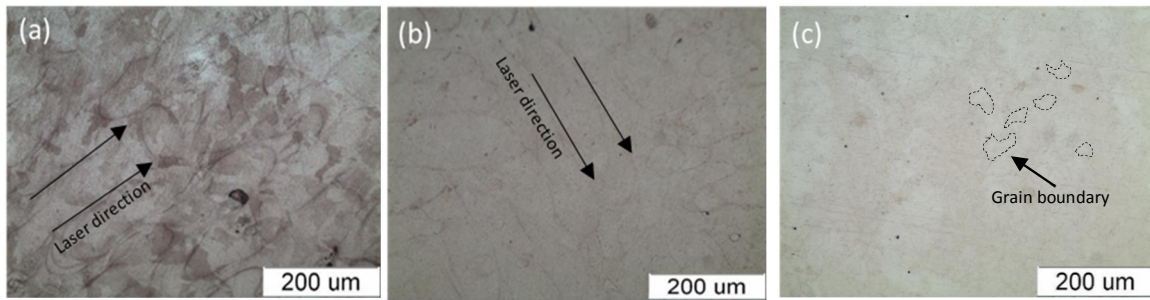
Figure 20. Surface structure of the STS 361L block samples. (a) As-built, (b) HT1, (c) HT2

4.3.2. Mechanical properties

Vickers micro-hardness measurements was performed in the block samples at as-build condition and after heat treatment. The average hardness of samples was presented in Table 6. At as-build condition, the hardness of 224 ± 8 HV was measured. After annealing at 650°C and 950°C for 2 hours, the hardness of the samples was decreased. HT1, which was applied a heat treatment at 650°C, the hardness of the sample was 211 ± 10 HV. HT2, which was applied a heat treatment at 650°C, the hardness of the sample was 205 ± 9 HV.

Table 6. Result of Hardness Testing

Condition	As built	HT1	HT2
Hardness (HV)	224 ± 8	211 ± 10	205 ± 9

The tensile test was conducted on the as-build and heat treatment samples. The result experiments were obtained and listed in Table 7. Figure 21 and Figure 22 represent the stress-strain curve for the as-built and heat-treated sample printed in the horizonal and vertical from substrate. From the data, we can observe that there were significant changes in the mechanical properties of printed samples after heat treatment. It is obvious to see that yield strength of the heat-treated samples decreased when the heat treatment temperature increased. This means the elastic region of the printed sample decreased after heat treatment. The ultimate tensile strength (UTS) of X-HT1 samples was higher than X-HT2 and similar with X-As built samples. With vertical orientation samples, the UTS of the heat-treated samples was lower than the as-built samples and the UTS of X-HT2 was higher than X-HT1. The elongation of the heat-treated samples was higher than the as-built samples. The region of plastic deformation is higher which show that the printed samples are more ductile after heat treatment.

The horizonal orientation and vertical orientation printed samples also showed significant differences

in the mechanical properties under the same test conditions. The strength values of X-As built samples were lower than Z-As built samples. However, the yield strength and UTS of X-HT1, X-HT2 were higher than Z-HT1, Z-HT2. The elongation of X-As built, X-HT1, X-HT2 were lower than Z-As built, Z-HT1, Z-HT2, respectively. This mean than the vertical orientation printed parts were more ductile than the horizonal orientation printed parts. And the plastic region of the horizonal orientation printed parts was higher than vertical orientation printed parts after heat treatment.

Table 7. Tensile test results

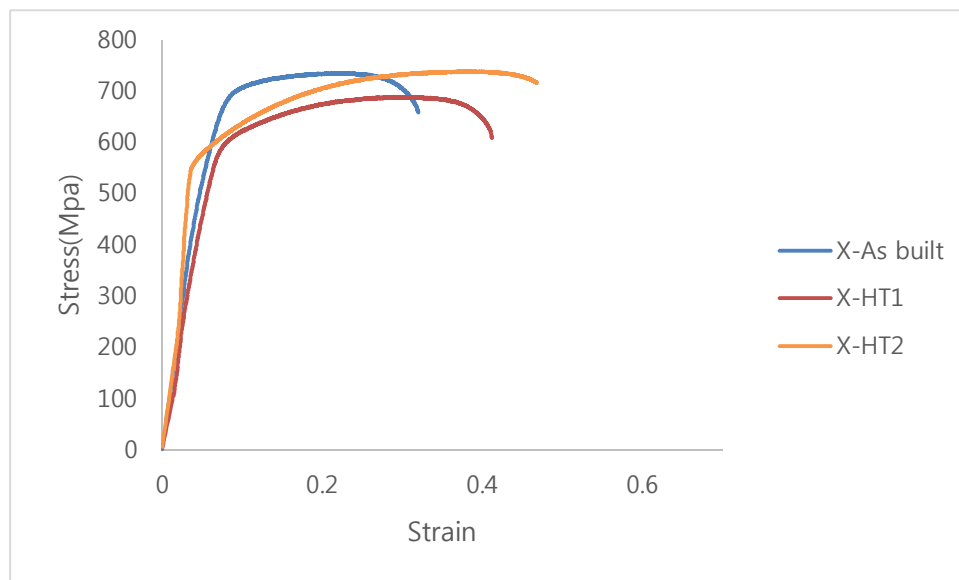| Condition	Yield strength (MPa)	UTS (MPa)	Elongation (%)
Horizonal orientation			
X-As built	680.78	734.80	32.20
X-HT1	585.90	688.58	41.53
X-HT2	578.34	738.29	49.27
Vertical orientation			
Z-As built	785.07	831.58	48.60
Z-HT1	533.04	574.23	50.57
Z-HT2	472.55	608.93	61.13

Figure 21. Stress-Strain curve for horizontal orientation printed samples
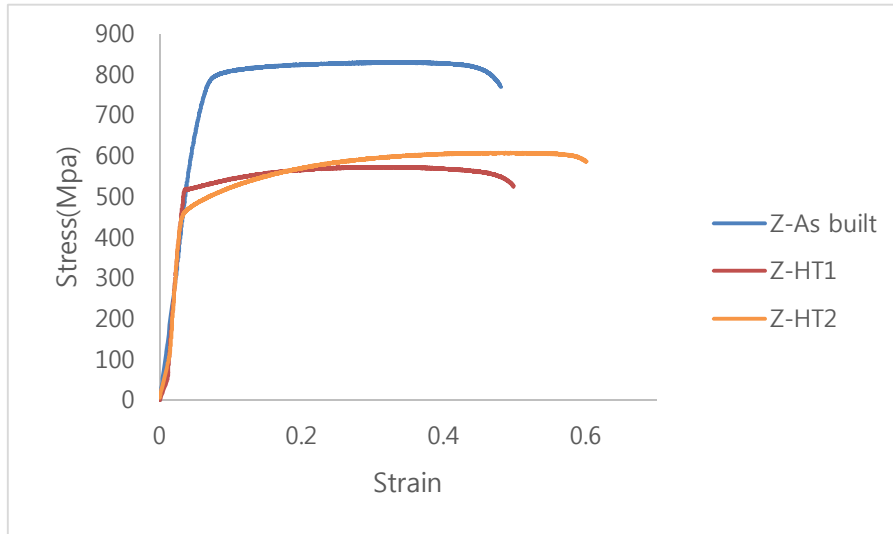
Figure 22. Stress-Strain curve for vertical orientation printed samples

The fracture surfaces of the samples were analyzed in order to understand mechanical properties under the test conditions. Figure 23 showed the fracture of tensile samples which were printed in horizontal and vertical orientation before and after the different heat treatments. The dimple structure and non-molten particles can be observed in all heat-treated samples. Z-HT1, Z-HT samples presented uniform dimple structure mor than X-HT1, X-HT2 which could explain the more ductility of vertical orientation printed samples than horizontal orientation printed samples.

Figure 23. SEM of surface fracture of the tensile samples

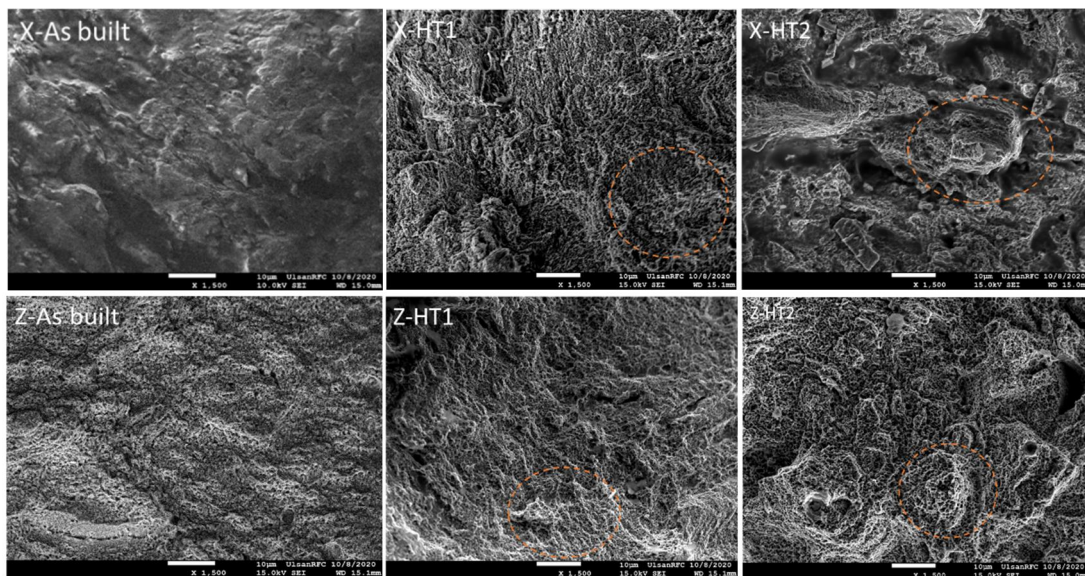## 5.13. 4.4. Conclusions

This study has presented the mechanical porosities of 316 stainless steel samples fabricated by SLM technical. Experimental works have been conducted with a purpose to study relationship between print orientations and heat treatment with the resultant microstructure and mechanical characterization. The as-built samples were fabricated with high relative density (>99%). There was no information of pores in the heat treatment stage. The hardness of SLM samples decreased with increasing of heat treatment temperature.

The yield strength and ultimate tensile strength declined after heat treatment due to decrease in the elastic region and dislocation density. The ultimate tensile strength of samples X-HT2 is higher than X-As built samples while the UTS of other samples decrease after heat treatment. Improved ductility with elongation at fracture from 30% to 60% was achieved after heat treatment. And, the vertical orientation printed parts show a higher ductility than horizontal orientation printed parts.

CHAPTER 5 – SUMMARY AND CONCLUSION

Recently, additive manufacture (AM) has been a major area of research because of its promising application in the rapid prototyping process of polymers, metals and ceramics and the ability to manufacture complex forms traditionally unrealized. In several methods such as stereo lithography, in polymers, the construction method can be used in layer-by-layer processes to fuse powdered material, for example select laser melting in metals. Metals are promising venue for SLM, as processing can optimize aeronautical industry weight and mechanical performances and 316L stainless steel has high corrosion and biomedical biocompatibility [60],[61].

The mechanical properties and microstructures have been extensively investigated based on system parameters, printing parameters and various materials since selective laser melting types of additive manufacture have been introduced [62]. For SLM metals, laser strength, scanning speed, hatch spacing, and manufacturing orientation form the key variable parameters. These parameters combined affect porosity, microstructure, and development of defects. The three inherent defects in SLM solidification are binding defects, gas pores and vacuums [63]. 316L stainless steel samples show that the laser power is the densest and almost completely dense (> 98% density) components have higher tensile strengths and elongations than bulk 316L material.

There are mainly some conclusions in this report that can be taken from this analysis on 316L stainless steel produced by additive manufacturing process:

- The appropriate 144W laser power and 750 mm / s laser speed illustrate the promising features and properties of 316L stainless steel printing.
- In the heat treatment process, there was no information about pores.
- After heat treatment, the yield strength and ultimate tensile strength decreased as the elastic area and dislocation density decreased.
- The printed parts of the vertical orientation exhibit greater ductility than the printed parts of the horizontal orientation.

REFERECES

1. "3D printing scales up". The Economist. 5 September 2013.

2. Excell, Jon (23 May 2010). "The rise of additive manufacturing". The Engineer. Retrieved 30 October 2013.

3. "Learning Course: Additive Manufacturing – Additive Fertigung". tmg-muenchen.de.

4. Most used 3D printing technologies 2017–2018 | Statistic". Statista. Retrieved 2 December 2018.

5. Jacobs, Paul Francis (1 January 1992). Rapid Prototyping & Manufacturing: Fundamentals of Stereolithography. Society of Manufacturing Engineers. ISBN 978-0-87263-425-1.

6. Azman, Abdul Hadi; Vignat, Frédéric; Villeneuve, François (29 April 2018). "Cad Tools and File Format Performance Evaluation in Designing Lattice Structures for Additive Manufacturing". Jurnal Teknologi. 80 (4). doi:10.11113/jt.v80.12058. ISSN 2180-3722.

7. "3D Printing Pens". yellowgurl.com. Archived from the original on 16 September 2016. Retrieved 9 August 2016.

8. "Model Repair Service". Modelrepair.azurewebsites.net. Retrieved 4 January 2016.

9. "Magics, the Most Powerful 3D Printing Software | Software for additive manufacturing". Software.materialise.com. Retrieved 4 January 2016.

10. "netfabb Cloud Services". Netfabb.com. 15 May 2009. Retrieved 4 January 2016.

11. Satyanarayana, B.; Prakash, Kode Jaya (2015). "Component Replication Using 3D Printing Technology". Procedia Materials Science. Elsevier BV. 10: 263–269. doi:10.1016/j.mspro.2015.06.049. ISSN 2211-8128.

12. "Objet Connex 3D Printers". Objet Printer Solutions. Archived from the original on 7 November 2011. Retrieved 31 January 2012.

13. "Design Guide: Preparing a File for 3D Printing" (PDF). Xometry.

14. "How to Smooth 3D-Printed Parts". Machine Design. 29 April 2014.

15. Delfs, P.; Ṫows, M.; Schmid, H.-J. (October 2016). "Optimized build orientation of additive manufactured parts for improved surface quality and build time". Additive Manufacturing. 12: 314–320. doi:10.1016/j.addma.2016.06.003. ISSN 2214-8604.

16. Haselhuhn, Amberlee S.; Gooding, Eli J.; Glover, Alexandra G.; Anzalone, Gerald C.; Wijnen, Bas; Sanders, Paul G.; Pearce, Joshua M. (2014). "Substrate Release Mechanisms for Gas Metal Arc Weld 3D Aluminum Metal Printing". 3D Printing and Additive Manufacturing. 1 (4): 204. doi:10.1089/3dp.2014.0015. S2CID 135499443.

17. Haselhuhn, Amberlee S.; Wijnen, Bas; Anzalone, Gerald C.; Sanders, Paul G.; Pearce, Joshua M. (2015). "In situ formation of substrate release mechanisms for gas metal arc weld metal 3-D

printing". Journal of Materials Processing Technology. 226: 50. doi:10.1016/j.jmatprotec.2015.06.038.

18. "Additive manufacturing – General Principles – Overview of process categories and feedstock". ISO/ASTM International Standard (17296–2:2015(E)). 2015.

19. "Standard Terminology for Additive Manufacturing – General Principles – Terminology". ASTM International – Standards Worldwide. 1 December 2015. Retrieved 23 August 2019.

20. Woern, Aubrey; Byard, Dennis; Oakley, Robert; Fiedler, Matthew; Snabes, Samantha (12 August 2018). "Fused Particle Fabrication 3-D Printing: Recycled Materials' Optimization and Mechanical Properties". Materials. 11 (8): 1413. Bibcode:2018Mate...11.1413W. doi:10.3390/ma11081413. PMC 6120030. PMID 30103532.

21. "Multi Jet Fusion (MJF) by HP".

22. The Third Wave, CNC, Stereolithography, and the end of gun control". Popehat. 6 October 2011. Retrieved 30 October 2013.

23. Rosenwald, Michael S. (25 February 2013). "Weapons made with 3-D printers could test gun-control efforts". Washington Post.

24. Zopf, David A.; Hollister, Scott J.; Nelson, Marc E.; Ohye, Richard G.; Green, Glenn E. (2013). "Bioresorbable Airway Splint Created with a Three-Dimensional Printer". New England Journal of Medicine. 368 (21): 2043–5.

25. Cobb, Harold M. (2010). The History of Stainless Steel. Materials Park, OH: ASM International. ISBN 9781615030118. Retrieved 8 March 2020.

26. Cobb, Harold M. (2010). The History of Stainless Steel. Materials Park, OH: ASM International. ISBN 9781615030118. Retrieved 8 March 2020.

27. ISSF Staff (8 March 2020). "The Stainless Steel Family" (PDF). Brussels, Belgium: International Stainless Steel Forum. p. 1, of 5. Retrieved 8 March 2020.

28. Chapter 05: Corrosion Resistance of Stainless Steels https://www.imoa.info/download_files/stainless-steel/issf/educational/Module_05_Corrosion_Resistance_of_Stainless_Steels_en.pdf

29. Stainless steels for design engineers (#05231G). https://www.asminternational.org/search/-/journal_content/56/10192/05231G/PUBLICATION: ASM International. 2008. pp. 69–78 (Chapter 6). ISBN 978-0-87170-717-8.

30. "Microstructures in Austenitic Stainless Steels :: Total Materia Article". www.totalmateria.com. Retrieved 23 June 2020.

31. Habara, Yasuhiro. Stainless Steel 200 Series: An Opportunity for MnArchived 8 March 2014 at the Wayback Machine. Technical Development Dept., Nippon Metal Industry, Co., Ltd.

32. "Welding of stainless steels and other joining methods" (PDF). Nickel Institute.

33. Shaigan, Nima; Qu, Wei; Ivey, Douglas; Chen, Weixing (2010). "A review of recent progress in coatings, surface modifications and alloy developments for solid oxide fuel cell ferritic stainless steel interconnects". Journal of Power Sources. Elsevier B.V. 195 (6): 1529–1542. Bibcode:2010JPS...195.1529S. doi:10.1016/j.jpowsour.2009.09.069.

34. "Stainless teel in Micro Hydro turbines". International Stainless Steel Forum. Archived from the original on 21 December 2019.

35. Hamano S., Shimizu T., Noda Toshiharu (2007). "Properties of Low Carbon High Nitrogen Martensitic Stainless Steels". Materials Science Forum. 539–543: 4975–4980. doi:10.4028/www.scientific.net/MSF.539-543.4975. S2CID 136518814.

36. Lacombe, P.; Baroux, B.; Beranger, G. (1990). Les Aciers Inoxydables. Les Editions de Physique. ISBN 2-86883-142-7.

37. "Chapter 5 corrosion resistance of stainless steels". www.worldstainless.org.

38. Specialty Steel Industry of North America (SSINA), Frequently asked questions, retrieved 6 April 2017.

39. "What is Stainless Steel?". Archived from the original on 24 September 2006. Retrieved 31 December 2005. nickelinstitute.org

40. "Stainless steel Reinforcing Bar: Applications". stainlesssteelrebar.org. 2019. Retrieved 28 January 2019.

41. By OKFoundryCompany from Richmond, USA - 84530877_FillingSys, CC BY 2.0, https://commons.wikimedia.org/w/index.php?curid=33067973

42. "DMLS | Direct Metal Laser Sintering | What Is DMLS?". Atlantic Precision.

43. "Direct Metal Laser Sintering". Xometry.

44. "Direct Metal Laser Sintering DMLS with ProtoLabs.com". ProtoLabs.

45. "How Direct Metal Laser Sintering (DMLS) Really Works". 3D Printing Blog | i.materialise. 8 July 2016.

46. Larry Greenemeier (9 November 2012). "NASA Plans for 3-D Printing Rocket Engine Parts Could Boost Larger Manufacturing Trend". Scientific American. Retrieved 13 November 2012.

47. Aboulkhair, Nesma T.; Everitt, Nicola M.; Ashcroft, Ian; Tuck, Chris (October 2014). "Reducing porosity in AlSi10Mg parts processed by selective laser melting". Additive Manufacturing. 1–4: 77–86. doi: 10.1016/j.addma.2014.08.001.

48. "Additive Companies Run Production Parts". RapidToday. Retrieved 12 August 2016.

49. Czichos, Horst (2006). Springer Handbook of Materials Measurement Methods. Berlin: Springer. pp. 303–304. ISBN 978-3-540-20785-6.

50. Davis, Joseph R. (2004). Tensile testing (2nd ed.). ASM International. ISBN 978-0-87170-806-9.

51. Davis 2004, p. 33.

52. Public Domain, https://commons.wikimedia.org/w/index.php?curid=1819661

53. H. Hauser, Inf_ J. Powder Met. 3, 7 (1967)

54. O. Grey, K. Beddow, Powder Technol, 2, 323 (1969)

55. B. Liu, R. Wildman, C. Tuck, I. Ashcroft, R. Hague, ResearchGate (2011)

56. R. Engeli, T. Etter, S. Hövel, K. Wegener, Mater. Process. Technol., 229, 484-491 (2016)

57. N.Kamariah, W. Harun, F. Ahmad, F.Tarlochan, Int. J. Manuf. Mater. Mech. Eng. 1, 01-18 (2020)

58. J. Collins (2018) https://doi.org/10.2144/000112517

59. A. Schneider, S. Rasband, W. Eliceiri, Nat. Methods 9, pages671–675 (2012)

60. Hao, et al. "Selective Laser Melting of a Stainless Steel and Hydroxyapatite Composite for Load-Bearing Implant Development." Journal of Materials Processing Tech., vol. 209, no. 17, 2009, pp. 5793–5801

61. Liverani, et al. "Effect of Selective Laser Melting (SLM) Process Parameters on Microstructure and Mechanical Properties of 316L Austenitic Stainless Steel." Journal of Materials Processing Tech., vol. 249, 2017, pp. 255–263.

62. Simchi, and Pohl. "Effects of Laser Sintering Processing Parameters on the Microstructure and Densification of Iron Powder." Materials Science &Amp; Engineering A, vol. 359, no. 1, 2003, pp. 119–128.

63. Cherry, J., et al. "Investigation into the Effect of Process Parameters on Microstructural and Physical Properties of 316L Stainless Steel Parts by Selective Laser Melting." The International Journal of Advanced Manufacturing Technology, vol. 76, no. 5, 2015, pp. 869–879.